Spin State Selective Detection of Single Quantum Transitions Using Multiple Quantum Coherence: Simplifying the Analyses of Complex NMR Spectra

Bikash Baishya[†] and N. Suryaprakash*[,‡]

Solid State and Structural Chemistry Unit and NMR Research Centre, Indian Institute of Science, Bangalore 560 012, India

Received: February 12, 2007; In Final Form: April 26, 2007

NMR spectra of molecules oriented in liquid-crystalline matrix provide information on the structure and orientation of the molecules. Thermotropic liquid crystals used as an orienting media result in the spectra of spins that are generally strongly coupled. The number of allowed transitions increases rapidly with the increase in the number of interacting spins. Furthermore, the number of single quantum transitions required for analysis is highly redundant. In the present study, we have demonstrated that it is possible to separate the subspectra of a homonuclear dipolar coupled spin system on the basis of the spin states of the coupled heteronuclei by multiple quantum (MQ)−single quantum (SQ) correlation experiments. This significantly reduces the number of redundant transitions, thereby simplifying the analysis of the complex spectrum. The methodology has been demonstrated on the doubly ^{13}C labeled acetonitrile aligned in the liquid-crystal matrix and has been applied to analyze the complex spectrum of an oriented six spin system.

Introduction

Analyses of NMR spectra of oriented molecules provide homo- and heteronuclear dipolar couplings and thereby molecular structure and order parameter.[1−4] Thermotropic nematic liquid crystals commonly used as solvents for such studies act as strong orienting media. Although the order parameter of the solute is an order of magnitude lower than that of the liquid-crystal solvent, it is still significantly large resulting in residual dipolar couplings (D_{IJ}), which are comparable to chemical shift (ν_I) differences. Thus, the resulting spectra correspond to that of strongly coupled spins. Furthermore, the spectral complexity increases rapidly with the increase in the number of interacting spins. As an example, in an oriented six spin system, there will be 792 theoretically allowed transitions, out of which 6 chemical shifts, 15 indirect spin−spin couplings, and 15 dipolar couplings are to be determined. In molecules with chemically or magnetically equivalent spins, the number of transitions is reduced, namely, oriented benzene with all the protons being chemically equivalent provides 76 transitions from which only three indirect and three direct dipolar couplings are to be determined. Thus, single quantum (SQ) transitions are highly redundant. Furthermore, the first-order analyses of the dipolar coupled spectra are generally not possible and one has to diagonalize the Hamiltonian numerically, adapting the least-square techniques. When the spectra are very complex and the starting parameters are far from real values, the iterative analysis can get captured in the local minimum, making further analysis very tedious. Several techniques are available in the literature either to reduce the complexity of the spectrum so that it is amenable for the first-order analyses or to derive additional information to aid the analyses of the complex spectra, namely, Z-COSY technique,[5] use of natural abundance ^2H NMR,[6] use of liquid crystals with low-order parameters,[7] higher order multiple quantum transitions,[8−11] use of multiple pulse sequences,[12−15] specific deuteration,[16] use of two-dimensional inverse experiments,[17−19] low-order orientation using bicelles,[20] and use of Lee Goldburg decoupling.[21] Though the application of the above techniques has been demonstrated on several spin systems, each of the above technique has its own limitations and is not routinely employed. Thus, the studies are restricted to eight interacting spins, beyond which the spectra become too complex and the analysis is tedious. However, there are reported studies in the literature on systems with more than 10 interacting spins.[22−24] Automatic analyses[25−32] of the spectra have also been developed which do not require any line assignments. Because of several limitations, automatic analysis is not routinely employed and most of the published works in the literature utilize computer program requiring manual interaction proving it to be more robust.

Another approach would be to reduce the redundancy in the single quantum transitions and to detect only required number of transitions for the spectral analysis. This direction has not been explored in the literature. The present study is on heteronuclear systems wherein we have employed homonuclear multiple quantum (MQ) coherence for selectively detecting the single quantum (SQ) transitions, in the proton spectrum, on the basis of the spin state of the coupled heteronuclear spin. The technique is demonstrated on the doubly ^{13}C labeled acetonitrile aligned in the liquid-crystalline phase and is extended to the analysis of the complex six spin proton spectra of orthodifluorobenzene aligned in the liquid-crystalline phase. However, the methodology can be employed both in the oriented and isotropic phases and not only for heteronuclear systems containing abundant spins like ^{19}F and ^{31}P but also for other labeled rare spins like ^{15}N, ^{13}C, and so forth.

Experimental Section

The solute molecules acetonitrile and orthodifluorobenzene obtained from Sigma Aldrich were used without further purification. The chemical structure and numbering of these

* To whom correspondence should be addressed. E-mail: nsp@sif.iisc.ernet.in.
[†] Solid State and Structural Chemistry Unit.
[‡] NMR Research Centre.

10.1021/jp071187k CCC: $37.00
Published on Web 05/27/2007

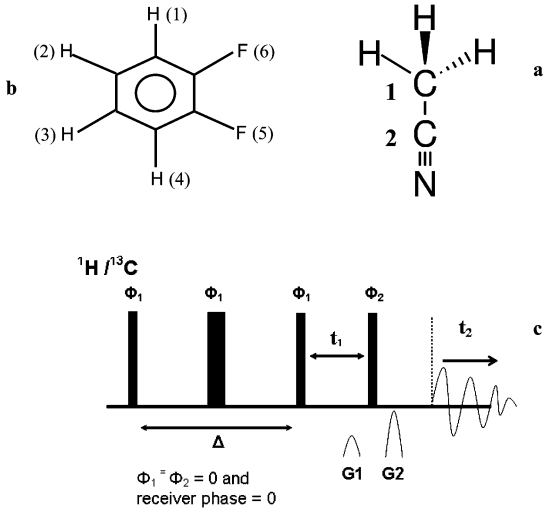

Figure 1. (a) The structure and numbering of interacting spins in doubly labeled acetonitrile. (b) The structure and numbering of interacting spins in orthodiflurobenzene. (c) The pulse sequence used for multiple quantum−single quantum correlation experiments. The delay Δ was optimized for the selection of proton and carbon homonuclear multiple quanta. The phases of all the pulses and the receiver were set to zero. The gradient ratio was set to G2 = *n*G1 for homonuclear *n*th quantum of proton and carbon.

molecules are shown in Figure 1a and 1b. The liquid-crystal ZLI-1132 was obtained from Merck. About 5% by weight of the samples were prepared in the liquid-crystal ZLI-1132. The homogeneous solutions of these samples have a line width of less than 10 Hz in the proton spectrum of acetonitrile and less than 5 Hz in the proton spectrum of orthodifluorobenzene. For acetonitrile studies, all the spectra were recorded on a Bruker AV-700 NMR spectrometer with field strength of 16.45 T operating at frequencies of 700.13 and 175.77 MHz for ^{1}H and ^{13}C nuclei, respectively. The enhanced sensitivity of the cryo probe reduced the experimental time significantly. The temperature used was maintained at 300 K by a Bruker BVT-3000 temperature regulating system. The samples were not spun during data acquisition.

The pulse sequence given in Figure 1c was used for all the 2D multiple quantum experiments. The delay, Δ, between the first and the second 90° pulse is optimized to get homonuclear antiphase magnetization. This value is 104 μs for triple quantum (TQ) and double quantum (DQ) of protons and 770 μs for DQ of carbons. The 180° pulse at the middle of the first two 90° pulses ensures that $J_{HH} + D_{HH}$ and $J_{CC} + 2D_{CC}$ evolves, respectively, for homonuclear proton and for homonuclear carbon MQ experiments. The second 90° pulse converts the antiphase magnetization into multiple quantum order. The particular multiple quantum order selected by the application of the gradients before and after the third 90° pulse converts this into observable single quantum transitions.

For the 2D experiment correlating homonuclear proton TQ coherence to its SQ coherence in acetonitrile, a data set consisting of 6 k and 512 points in F2 (single quantum) and F1 (multiple quantum) dimensions, respectively, was chosen. Spectral widths of 24 k and 76 k were chosen in the direct and indirect dimensions, respectively. The number of accumulations was two for each t_1 increment. Relaxation delay used was 3.5 s. The time domain data was processed by zero filling it to 8 k and 1 k points in F1and F2 dimensions, respectively, without any window function and linear prediction. The spectrum was displayed in magnitude mode with a digital resolution of 2.93 and 74.19 Hz in the direct and indirect dimensions, respectively.

For the 2D experiment correlating homonuclear carbon DQ coherence to its SQ coherence in acetonitrile, a data set consisting of 6 k and 256 points in F2 and F1 dimensions, respectively, was chosen. Spectral widths of 45 k and 90 k were chosen in the direct and indirect dimensions, respectively. The number of accumulations was six for each t_1 increment. Relaxation delay was 3.5 s. The time domain data was linear predicted to 512 points and was zero filled to 8 k and 1 k points in SQ and MQ dimensions, respectively, and was processed without any window function. The spectrum is displayed in magnitude mode with a digital resolution of 5.54 and 87 Hz in the direct and indirect dimensions, respectively.

For the 2D experiment correlating homonuclear DQ coherence of proton to its SQ coherence, a data set consisting of 6 k and 512 points in F2 and F1 dimensions, respectively, was chosen. Spectral widths of 24 k and 55 k were chosen in the direct and indirect dimensions, respectively. The number of scans was 2 for each t_1 increment. Relaxation delay was 3.5 s. The time domain data was linear predicted to 512 points and was zero filled to 8 k and 2 k points in SQ and MQ dimensions, respectively, and was processed without any window function. The spectrum is displayed in magnitude mode with a digital resolution of 2.93 and 26.84 Hz in the direct and indirect dimensions, respectively.

For orthodifluorobenzene studies, all the spectra were recorded on a Bruker DRX-500 NMR spectrometer operating at the field strength of 11.3 T corresponding to resonance frequencies of 500.13 and 125.77 MHz for ^{1}H and ^{13}C nuclei, respectively, using BBI probe. The acquisition mode in the indirect dimension was with quadrature off. To ensure the creation of MQ coherence, the offset was set to one end of the spectrum in all the MQ experiments. Only the spectral region of interest was plotted.

For the two-dimensional experiment correlating homonuclear fourth quantum (FQ) coherence of protons to its SQ coherence, a data set consisting of 4 k and 256 points in F2 and F1 dimensions, respectively, were chosen. Spectral widths of 13 k and 48 k were chosen in the direct and indirect dimensions, respectively. The optimized delay Δ was 250 μs. The number of accumulations was 32 for each t_1 increment. Relaxation delay was 3.5 s. The time domain data was linear predicted to 512 points and was processed by zero filling to 8 k and 1 k points in F2 and F1 dimensions, respectively, without using any window function. The spectrum is displayed in magnitude mode with a digital resolution of 3.17 and 46.86 Hz in the SQ and MQ dimensions, respectively.

Results and Discussion

Multiple Quantum NMR. The different multiple quantum orders of N interacting spins can be selectively excited[33] or detected.[34] The number of allowed transitions for the mth order spectrum of N interacting spins is given by

$$2N!/(N - m)!\,(N + m)!\,... \qquad (1)$$

Thus, for the highest quanta, namely, when $N = m$, there is only one allowed transition. This corresponds to a situation when all the spins flip at a time from the state $|\alpha\rangle$ to the state $|\beta\rangle$ or vice versa. The spins then evolve only under chemical shifts and do not evolve under the direct or indirect spin−spin couplings. The highest quantum spectrum, therefore, provides information only on the sum of all the chemical shifts. N-1 quantum is a situation in which N-1 spins flip (active spins) in the presence of one leftover spin (a passive spin). Thus, N-1 quantum spectrum provides a doublet centered at the sum of

the chemical shift positions of the active spins whose separation provides the sum of the couplings of the passive spins to the active spins. The *N*-2 quantum spectrum is a situation where two spins flip at a time in the presence of the remaining spins. This will have more transitions than *N*-1 quantum but significantly less compared to SQ transitions. The number of transitions and thereby the complexity of the spectrum decreases by going to higher quantum. Also, for oriented molecules, *N*-1 and *N*-2 quantum spectra are sufficient to derive information on all the dipolar couplings,[35,36] thereby indicating that the SQ transitions are highly redundant.

Multiple Quantum (MQ)−Single Quantum (SQ) Correlation. The transfer of the MQ coherence to the observable SQ for different types of spin systems[37] and the flip angle dependence of the intensities for an AMX have been discussed earlier.[38] In the schematic representation of the correlation of DQ coherence to its SQ coherence on a homonuclear *J* coupled AMX spin system,[37] the DQ dimension provides three doublets with the separation corresponding to the sum of the *J*-couplings between the passive spins and the active spins centered at the sum of the chemical shift positions of the two active spins. Each of these doublets corresponds to the states $|\alpha\rangle$ and $|\beta\rangle$ of the passive spin. The cross sections taken along the SQ dimension for each spin state of the passive spin give all the 12 transitions expected for an AMX spin system, whose intensities depend on the flip angle. Thus, the application of a nonselective mixing pulse results in each $|\alpha\rangle$ and $|\beta\rangle$ state of A, M, and X spins correlating to all the allowed transitions in the SQ dimension. If, on the other hand, a selective pulse is applied only on the active spins and no pulse is applied on the passive spins, then the state of the passive spins remains the same both in MQ and SQ dimensions. Each state of the passive spins in the MQ dimension then encodes the spin states involved in the SQ transitions that arise only because of coupling between active spins. This results in the selective detection of SQ transitions. The cross section taken along SQ dimension for any one of the passive spin states has sufficient number of transitions essential to determine the couplings between active spins. This reduces the redundant transitions and simplifies the complexity of the spectrum.

Doubly Labeled Acetonitrile ($^{13}CH_3{}^{13}CN$). The protons and carbons of doubly ^{13}C labeled acetonitrile, aligned in the liquid crystal, form a spin system of the type A_3MX. The ^1H SQ spectrum gives a 1:2:1 triplet because of D_{HH}, and each line of this triplet is further split into a doublet of doublets of equal intensity giving rise to a total of 12 transitions. D_{HH} and D_{CH} can be determined by the first-order analysis of this spectrum, which is straightforward.

For the MQ studies, the two types of heteronuclei in this molecule can be treated as two isolated systems. Thus, it was possible to selectively detect homonuclear DQ and TQ orders between protons and homonuclear DQ between carbons. The particular order was selected by using gradients[8] and the selected MQ coherence was allowed to correlate its SQ coherence. Depending on the order selectively detected, the MQ spectrum is analyzed treating it as spin systems such as AMX, A_3X, and APMX.

$^{13}CH_3{}^{13}CN$ as an AMX Spin System: Selective Detection of ^1H SQ Transitions Using Homonuclear Proton TQ Coherence. The active and the passive spins in the SQ and TQ dimensions and the energy-level diagram describing the connectivities of homonuclear proton triple quantum coherence to its single quantum coherence are shown in Figure 2. Figure 3 shows the 2D spectrum correlating the TQ coherence of protons

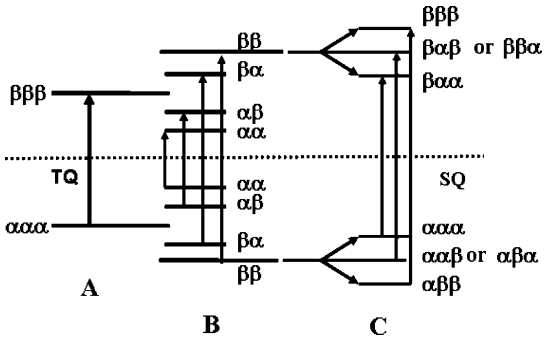

Figure 2. The energy-level diagram describing the connectivities of triple quantum to single quantum transitions; the dashed horizontal line separates the ground and the excited states. (A) Active homonuclear proton spin states involved in the triple quantum transitions and (B) passive heteronuclear spin states coupled to the triple quantum spin states of proton, i.e., $\alpha\alpha\alpha$ to $\beta\beta\beta$. For each of these two triple quantum states, there are four possible heteronuclear coupled spin states giving four possible transitions in the triple quantum dimension. (C) Single quantum transitions of protons in the direct dimension arising from the spin state selected triple quantum transitions giving rise to four cross sections. Each of these cross sections pertains to selectively detected SQ transitions originating from the initial third quantum state which has two carbons, in one of the $\alpha_{C1}\alpha_{C2}$, $\alpha_{C1}\beta_{C2}$, $\beta_{C1}\alpha_{C2}$, and $\beta_{C1}\beta_{C2}$ states, and which ends up in the states where single proton spin flips but still has carbons in its respective initial $\alpha_{C1}\alpha_{C2}$, $\alpha_{C1}\beta_{C2}$, $\beta_{C1}\alpha_{C2}$, and $\beta_{C1}\beta_{C2}$ state. The transitions arising from the initial and final states of the carbons in the $\beta_{C1}\beta_{C2}$ states are shown as an example. However, the similar transitions from $\alpha_{C1}\alpha_{C2}$, $\alpha_{C1}\beta_{C2}$, and $\beta_{C1}\alpha_{C2}$ give single quantum triplets in different cross sections. The TQ dimension provides information on D_{C1H} and D_{C2H} and the SQ dimension provides information on D_{HH}.

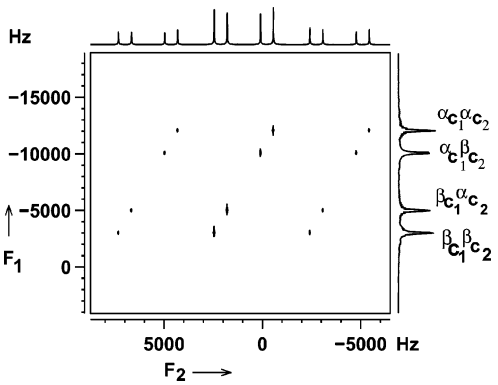

Figure 3. The 700 MHz 2D spectrum of acetonitrile in the liquid-crystal ZLI-1132, correlating proton TQ coherence to its SQ coherence. The $\alpha_{C1}\alpha_{C2}$, $\alpha_{C1}\beta_{C2}$, $\beta_{C1}\alpha_{C2}$, and $\beta_{C1}\beta_{C2}$ are different spin states of heteronuclei. The other experimental details are given in the text.

with its SQ coherence along with the corresponding projections. The excitation of proton TQ results in all the protons evolving at the sum of the resonance offset (chemical shifts can be treated as zero because of magnetic equivalence of all the three protons) under sum of J_{CH} and D_{CH} couplings in the MQ dimension. This pertains to a situation where the selective mixing pulse is applied on A and in the MQ dimension A_3MX spin system behaves like an AMX spin system, where the proton is the active spin (A) and the two carbons are the passive spins (M and X). The TQ spectrum corresponds to the A part of this AMX spectrum (Figure 2A). In the spin product basis set, the spin states of two weakly coupled M and X spins, coupled to triple quantum states of proton $|\alpha_P\alpha_P\alpha_P\rangle$ and $|\beta_P\beta_P\beta_P\rangle$, are written as $|\alpha_{C1}\alpha_{C2}\rangle$, $|\alpha_{C1}\beta_{C2}\rangle$, $|\beta_{C1}\alpha_{C2}\rangle$, and $|\beta_{C1}\beta_{C2}\rangle$, where the subscripts P, C1, and C2 correspond to protons and carbons of CH_3 and CN groups. The four transitions of the A spin in the TQ

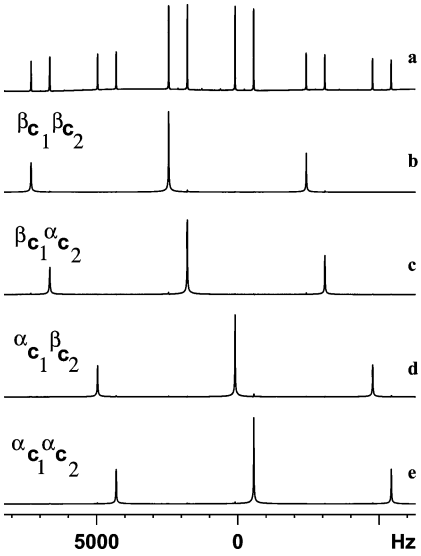

Figure 4. (a) The 700 MHz proton 1D spectrum of acetonitrile in the liquid-crystal ZLI-1132. (b−e) Cross sections along SQ dimension taken at the spin states $\beta_{C1}\beta_{C2}$, $\beta_{C1}\alpha_{C2}$, $\alpha_{C1}\beta_{C2}$, and $\alpha_{C1}\alpha_{C2}$ in TQ dimension, respectively. The other experimental details are given in the text.

dimension correspond to these four spin states (Figure 2B). The doublet separations between the states $|\alpha_{C1}\alpha_{C2}\rangle$ and $|\alpha_{C1}\beta_{C2}\rangle$ provide D_{C2H} and between the states $|\alpha_{C1}\alpha_{C2}\rangle$ and $|\beta_{C1}\alpha_{C2}\rangle$ provide D_{C1H}.

The spectrum in the SQ dimension is for an A_3MX type spin system and consists of four A_3 subspectra, one for each of the four *mI*(M and X) values of $|\alpha_{C1}\alpha_{C2}\rangle$, $\alpha_{C1}\beta_{C2}\rangle$, $\beta_{C1}\alpha_{C2}\rangle$, and $\beta_{C1}\beta_{C2}\rangle$, of the two carbons. For transition within each subspectrum, the spin state of M and X does not change. The Eigen values of Mz (= *I*z(X) + *I*z(M)) are to be considered as good quantum numbers and as a special rule for allowed A_3 lines it follows that $\Delta M_Z = 0$.

The 1D spectrum along with the cross sections taken on SQ dimension at different spin states of TQ dimension is shown in Figure 4a−4e. Each of these cross sections pertains to selectively detected SQ transitions originating from the initial third quantum state which has two carbons, either in $\alpha_{C1}\alpha_{C2}$ or $\beta_{C1}\beta_{C2}$ state, and which ends up in states where single proton spin flips but still has carbons in its initial $\alpha_{C1}\alpha_{C2}$ or $\beta_{C1}\beta_{C2}$ state. An example of such a transition is from the states $\alpha_P\alpha_P\alpha_P\beta_{C1}\beta_{C2}$ and $\beta_P\alpha_P\alpha_P\beta_{C1}\beta_{C2}$ (Figure 2C). This is because the last 90° pulse on protons does not alter the spin states of heteronuclei. Thus, all proton single quantum transitions pertaining to four A_3 subspectra get separated into different cross sections depending on the four spin states of the heteronuclei. Each cross section is a triplet, from which D_{HH} can be determined. Thus, as far as the determination of the D_{HH} is concerned, the redundancy in the number of transitions required for the analysis in the normal 1D spectrum is significantly reduced.

$^{13}CH_3{}^{13}CN$ as an A_3X Spin System: Spin State Selective Detection of ^{13}C SQ Transitions Using Homonuclear Carbon DQ Coherence. In the ^{13}C spectrum, the carbon M of the A_3-MX spin system is split into a quartet by three protons (A_3), each of which further splits into doublets because of weak coupling to the other carbon (spin X). Similarly, the carbon X is split into a quartet because of its coupling with protons (A_3), each transition of which is further split into doublets because of its weak coupling with the other carbon (spin M). The fully coupled ^{13}C spectrum, therefore, provides equal intensity doublets of 1:3:3:1 intensity quartets at the chemical shift positions of each carbon.

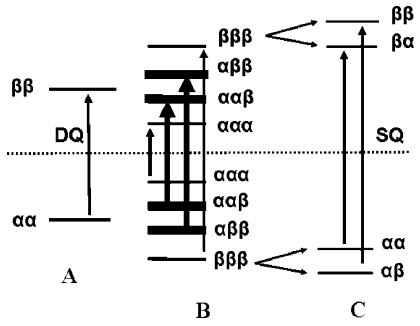

Figure 5. The energy-level diagram describing the connectivities of homonuclear carbon double quantum coherence to its single quantum coherence; the dashed horizontal line separates the ground and the excited states. (A) Active homonuclear carbon spin states, $\alpha_{C1}\alpha_{C2}$ and $\beta_{C1}\beta_{C2}$, involved in the double quantum transitions. (B) The double quantum states of two carbons coupled to eight different spin states, $\alpha_P\alpha_P\alpha_P$, $\alpha_P\alpha_P\beta_P$, $\alpha_P\beta_P\alpha_P$, $\beta_P\alpha_P\alpha_P$, $\alpha_P\beta_P\beta_P$, $\beta_P\beta_P\alpha_P$, $\beta_P\alpha_P\beta_P$, and $\beta_P\beta_P\beta_P$, of protons. The states $\alpha_P\alpha_P\beta_P$, $\alpha_P\beta_P\alpha_P$, and $\beta_P\alpha_P\alpha_P$ are degenerate and form one group. The states $\alpha_P\beta_P\beta_P$, $\beta_P\beta_P\alpha_P$, and $\beta_P\alpha_P\beta_P$ are degenerate and form another group. These two states are shown in thick horizontal bars. The thick vertical arrows show the degenerate transitions with 3 times more intensity than the other ones (C) Single quantum transitions of carbons in the direct dimension arising from the spin state selected double quantum transitions giving rise to four cross sections. Each of these cross sections pertains to selectively detected SQ transitions originating from the initial second quantum state which has three protons, in one of the $\alpha_P\alpha_P\alpha_P$, $\alpha_P\alpha_P\beta_P$, $\alpha_P\beta_P\alpha_P$, $\beta_P\alpha_P\alpha_P$, $\alpha_P\beta_P\beta_P$, $\beta_P\beta_P\alpha_P$, $\beta_P\alpha_P\beta_P$, and $\beta_P\beta_P\beta_P$ states, and which ends up in the states where single carbon spin flips but still has protons in its respective initial $\alpha_P\alpha_P\alpha_P$, $\alpha_P\alpha_P\beta_P$, $\alpha_P\beta_P\alpha_P$, $\beta_P\alpha_P\alpha_P$, $\alpha_P\beta_P\beta_P$, $\beta_P\beta_P\alpha_P$, $\beta_P\alpha_P\beta_P$, and $\beta_P\beta_P\beta_P$ states. The transitions arising from the initial and final states of the proton in the $\beta_P\beta_P\beta_P$ states are shown as an example. However, the similar transitions from other states give single quantum doublets in different cross sections. The DQ dimension provides information on D_{C1H} and D_{C2H} and the SQ dimension provides information on D_{C1C2}.

The active and the passive spins in the SQ and DQ dimensions and the energy-level diagram describing the connectivities of homonuclear carbon double quantum coherence to its single quantum coherence are shown in Figure 5. The DQ excitation of homonuclear carbon spins converts the five-spin system of the type A_3MX into an A_3X type in the DQ dimension, where the three protons are passive spins (A_3) and the two ^{13}C are active spins (X) (Figure 5A). The double quantum states of two carbons are $\alpha_{C1}\alpha_{C2}$ and $\beta_{C1}\beta_{C2}$, and they are coupled to eight different spin states, $\alpha_P\alpha_P\alpha_P$, $\alpha_P\alpha_P\beta_P$, $\alpha_P\beta_P\alpha_P$, $\beta_P\alpha_P\alpha_P$, $\alpha_P\beta_P\beta_P$, $\beta_P\beta_P\alpha_P$, $\beta_P\alpha_P\beta_P$, and $\beta_P\beta_P\beta_P$ of protons. The states $\alpha_P\alpha_P\beta_P$, $\alpha_P\beta_P\alpha_P$, and $\beta_P\alpha_P\alpha_P$ are degenerate and form one group. The states $\alpha_P\beta_P\beta_P$, $\beta_P\beta_P\alpha_P$, and $\beta_P\alpha_P\beta_P$ are degenerate and form another group (Figure 5B). This results in the splitting of the active spin transition into a quartet by passive spins in the DQ dimension (Figure 5B). Figure 6 shows the DQ coherence of carbon correlating to its SQ coherence along with the projections on DQ and SQ axis. Carbon 1, directly bonded to protons, resonates at high field and also has large D_{C1H}. Carbon 2, remotely bonded to protons, resonates at lower field and has small D_{C2H}. Furthermore, the resonance signal from carbon 2 is significantly broadened because of quadrupolar nitrogen, and the signals are very weak in intensity. Thus, only high-field region of the spectrum is given in Figure 6. The cross section taken along SQ dimension at each spin state of a passive spin in the MQ dimension is a doublet from which D_{CC} can be directly obtained. D_{C1H} can be determined from the combined analysis of any two consecutive cross sections. Similarly, the analysis of the low-field region of the spectrum provides D_{C2H}

$^{13}CH_3{}^{13}CN$ as an APMX Spin System: Spin State Selective Detection of ^1H SQ Transitions Using Homonuclear Proton

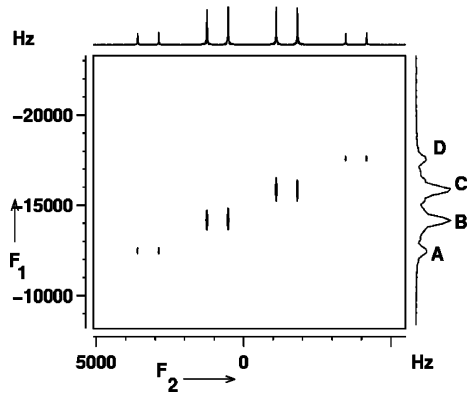

Figure 6. The 700 MHz 2D spectrum of homonuclear carbon double quantum coherence correlating to its single quantum coherence of acetonitrile in the liquid-crystal ZLI-1132. A and D correspond to spin states $\alpha_P\alpha_P\alpha_P$ and $\beta_P\beta_P\beta_P$, respectively, B and C correspond to degenerated spin states ($\alpha_P\alpha_P\beta_P$, $\alpha_P\beta_P\alpha_P$, $\beta_P\alpha_P\alpha_P$) and ($\alpha_P\beta_P\beta_P$, $\beta_P\beta_P\alpha_P$, $\beta_P\alpha_P\beta_P$), respectively. The other experimental details are given in the text.

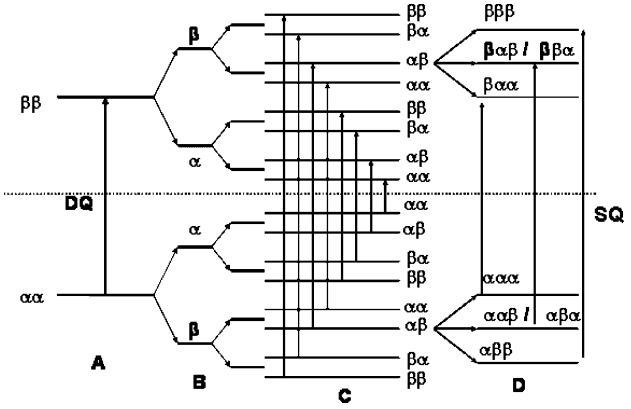

Figure 7. The energy-level diagram describing the connectivities of homonuclear proton double quantum to single quantum transitions; the dashed horizontal line separates the ground and the excited states in both dimensions. (A) Active homonuclear proton spin states involved in the double quantum transitions, (B) passive proton spin states coupled to active proton double quantum states, (C) further splitting of active double quantum protons spin states coupled to proton by two passive carbon spin states, and (D) the single quantum transitions arising from the passive spin states in the double quantum dimension. The transitions arising from the initial and final states of the passive heteronuclear spin in the $\alpha\beta$ states are shown as an example. However, the similar transitions from other states give single quantum triplets in different cross sections. The DQ dimension provides information on D_{C1H} and D_{C2H} and the SQ dimension provides information on D_{HH}.

DQ Coherence. The spin system of the type APMX is created in the DQ dimension when two protons are simultaneously flipped in the presence of two carbons and the third proton. Active spins for DQ could be any of the two protons of CH_3 group. The DQ dimension will then have a passive proton spin and two carbon spins. The entire spin system is a weakly coupled four-spin system of the type APMX, where A is the double quantum excited two protons of CH_3 (active spins) group, P is proton not participating in double quantum (passive spin), and M and X are two carbons (passive spins). The active and the passive spins in the SQ and DQ dimensions and the energy-level diagram describing the connectivities of homonuclear proton double quantum coherence to its single quantum coherence are shown in Figure 7. The weakly coupled four-spin system gives eight transitions for each spin. Thus, in the DQ dimension, A spin transition is split into eight transitions of equal intensity by the passive spins. The corresponding DQ coupled spin states of A are $\alpha_P\alpha_{C1}\alpha_{C2}\rangle$, $|\alpha_P\alpha_{C1}\beta_{C2}\rangle$, $|\alpha_P\beta_{C1}\alpha_{C2}\rangle$, $|\alpha_P\beta_{C1}\beta_{C2}\rangle$, $|\beta_P\alpha_{C1}\alpha_{C2}\rangle$, $|\beta_P\beta_{C1}\alpha_{C2}\rangle$, $|\beta_P\alpha_{C1}\beta_{C2}\rangle$, and $|\beta_P\beta_{C1}\beta_{C2}\rangle$. The 2D spectrum correlating DQ coherence of protons with its SQ coherence is shown in Figure 8. The cross section taken along SQ dimension for each spin state in the DQ dimension is a triplet from which D_{HH} can be determined.

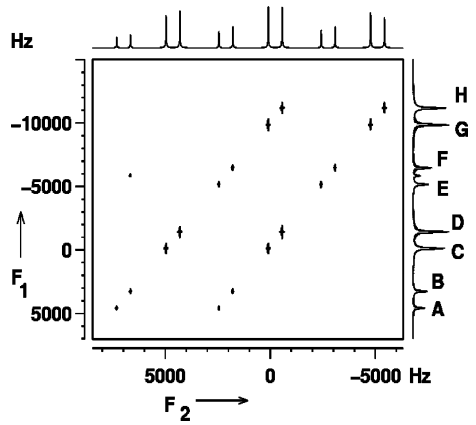

Figure 8. The 700 MHz 2D spectrum of acetonitrile in the liquid-crystal ZLI-1132, correlating homonuclear double quantum coherence of proton to its single quantum coherence. A−H correspond to spin states $\alpha_P\alpha_{C1}\alpha_{C2}$, $\alpha_P\alpha_{C1}\beta_{C2}$, $\alpha_P\beta_{C1}\alpha_{C2}$, $\alpha_P\beta_{C1}\beta_{C2}$, $\beta_P\alpha_{C1}\alpha_{C2}$, $\beta_P\beta_{C1}\alpha_{C2}$, $\beta_P\alpha_{C1}\beta_{C2}$, and $\beta_P\beta$-$_{C1}\beta_{C2}$, respectively. The other experimental details are given in the text.

The values of D_{HH}, D_{C1H}, D_{C2H}, and D_{CC} determined from the one-dimensional ^1H and ^{13}C spectrum are 1626.7, 1107.0, 334.8, and 357.5 Hz, respectively. These values agree with those measured from the 2D MQ experiments.

Study on an Oriented AA′BB′XX′ Spin System. The analysis of the spectrum of oriented acetonitrile discussed in the previous sections pertains to the weakly coupled spin system, and the first-order analysis of the 2D cross sections could be carried out to determine the spectral parameters. However, in general, the spin systems in the liquid-crystalline media being strongly coupled, the iterative analysis has to be carried out to derive the spectral parameters. This method is, therefore, applied to simplify the iterative analysis of ^1H spectrum of a six-spin system, orthodifluorobenzene aligned in liquid-crystal phase.

The structure and the numbering of the interacting spins in orthodifluorobenzene are shown in Figure 1b, forming a strongly coupled spin system of the type AA′BB′XX′, and the 2D spectrum which correlates the homonuclear fourth quantum (FQ) coherence of protons to its SQ coherence is given in Figure 9 along with the corresponding projections on SQ and FQ dimensions. Figure 10a−10d shows the one-dimensional proton spectrum of the molecule in the liquid-crystal ZLI-1132 along with the three cross sections taken along SQ of Figure 9. Each transition observed in the spectra 10b−10d is different from each other in frequency. However, there is a one-to-one overlap of all the transitions of the cross sections with the 1D proton spectrum of Figure 10a.

The gradient-selected proton homonuclear FQ excitation results in the flipping of all the protons and evolves under the sum of their chemical shifts and proton−fluorine dipolar couplings. This corresponds to AXX′ type in the FQ dimension, where A is the proton (active spin) and XX′ is two fluorines (passive spins). In the FQ dimension, the active spin A is split because of dipolar couplings with two passive spins. The XX′ part will have four possible spin states, namely, (a) $|\alpha_1\alpha_2\rangle$, (b) $(|\alpha_1\beta_2\rangle + |\beta_1\alpha_2\rangle)/\sqrt{2}$, (c) $(|\alpha_1\beta_2\rangle - |\beta_1\alpha_2\rangle)/\sqrt{2}$, and (d) $|\beta_1\beta_2\rangle$. The degenerate central transition arises from the spin states ($|\alpha\beta\rangle$

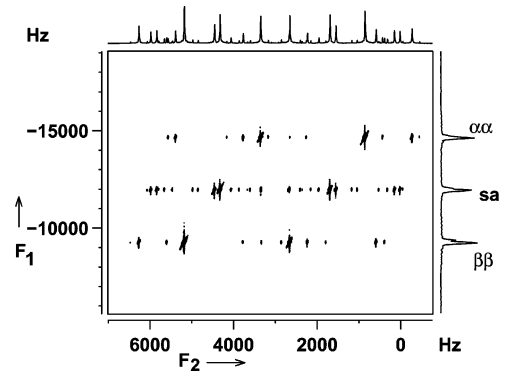

Figure 9. The 500 MHz 2D spectrum of orthodifluorobenzene aligned in the liquid-crystal ZLI-1132, correlating homonuclear FQ coherence of protons to its SQ coherence. Two outer transitions in the FQ dimension correspond to spin states $|\alpha\alpha\rangle$ and $|\beta\beta\rangle$, respectively, s and a refer to spin states $(|\alpha_1\beta_2\rangle + |\beta_1\alpha_2\rangle)/\sqrt{2}$ and $(|\alpha_1\beta_2\rangle - |\beta_1\alpha_2\rangle)/\sqrt{2}$, respectively. The other experimental details are given in the text.

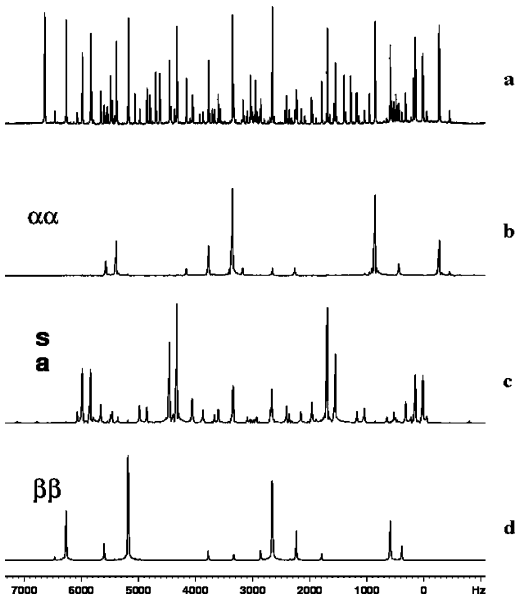

Figure 10. (a) The 500 MHz 1D proton spectrum of orthodifluorobenzene aligned in the liquid-crystalline phase ZLI-1132; (b−d) the FQ dimension of Figure 5B plotted with identical scale for comparison. s and a refer to symmetric and antisymmetric states $(|\alpha_1\beta_2\rangle + |\beta_1\alpha_2\rangle)/\sqrt{2}$ and $(|\alpha_1\beta_2\rangle - |\beta_1\alpha_2\rangle)/\sqrt{2}$, respectively. The other experimental details are given in the text.

$+ |\beta\alpha\rangle)/\sqrt{2}$ and $(|\alpha\beta\rangle - |\beta\alpha\rangle)/\sqrt{2}$. The other two outer transitions correspond to spins states $|\alpha\alpha\rangle$ and $|\beta\beta\rangle$.

The cross sections taken along the SQ dimension, at three different spin states in the FQ dimension, correspond to selectively detected single quantum transitions on the basis of the spin state of the passive spins. The selectively detected transitions at each cross section contain information on the proton chemical shifts and proton−proton dipolar couplings. The 12 SQ transitions are selectively detected for $|\alpha\alpha\rangle$ and $|\beta\beta\rangle$ states. The analysis of one of these is sufficient for the determination of proton chemical shifts and proton dipolar couplings. Thus, this significantly reduces the complexity of the analysis. Similar information can also be obtained using the SQ transitions that are selectively detected for the spin states $(|\alpha_1\beta_2\rangle + |\beta_1\alpha_2\rangle)/\sqrt{2}$ and $(|\alpha_1\beta_2\rangle - |\beta_1\alpha_2\rangle)/\sqrt{2}$ of fluorine, for which there are nearly 60 transitions.

The three selectively detected single quantum spectra were independently analyzed using the computer program LEQUOR.[39] The indirect spin−spin couplings taken from the literature[40] were kept constant during the iteration. Only proton dipolar couplings and proton chemical shifts were varied during the iteration, and all the 12 selectively excited transitions for $|\alpha\alpha\rangle$ and $|\beta\beta\rangle$ states were assigned to a root-mean-square error of 0.6 Hz in each analysis. Combined analyses of spectra from both $|\alpha\alpha\rangle$ and $|\beta\beta\rangle$ states also provide D_{HH} couplings. The analysis of the spectrum from the spin states $(|\alpha_1\beta_2\rangle + |\beta_1\alpha_2\rangle)/\sqrt{2}$ and $(-|\alpha_1\alpha_2\rangle + |\beta_1\alpha_2\rangle)/\sqrt{2}$ of fluorine provides D_{HH} and D_{FH} couplings. Although the D_{HH} could be determined with the same precision and the rms error was 0.6 Hz, the standard deviations for D_{FH} couplings were very large. The combined analysis of the spectra taken at the cross section for the spin state $|\alpha\alpha\rangle$ and the degenerate spin state was carried out. Forty-five lines were assigned to an rms error of 0.7 Hz. The standard deviations of the determined parameters, D_{HH} and D_{FH}, indicated that these parameters are very precise. To ascertain the precision of the determinacy of the spectral parameters, the SQ spectrum (Figure 10a) was also independently analyzed in a conventional way, and all the observed 83 transitions were assigned to a root-mean-square error of 0.08 Hz. The derived spectral parameters in all the above analyses are given in Figure 11 as a histogram.

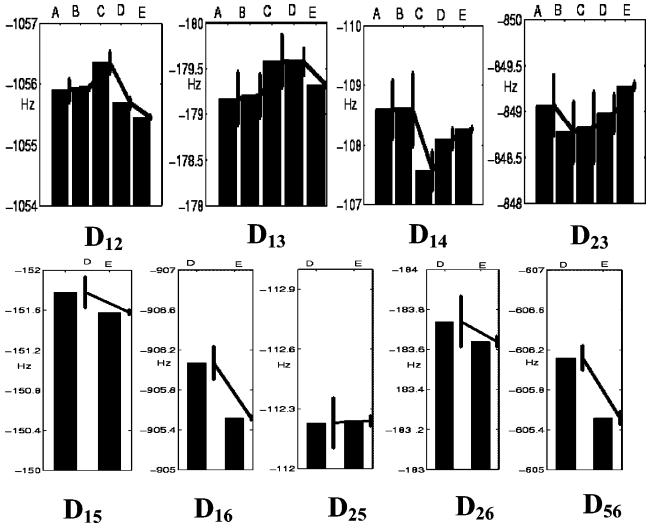

Figure 11. The histogram showing the values of dipolar couplings determined by the analyses of the different cross sections of the spectrum shown in Figure 9 and from the 1D proton spectrum. Top trace: homonuclear proton couplings obtained by (A) the analysis of the cross section taken along SQ dimension at the spin state $|\alpha\alpha\rangle$ in FQ dimension, (B) the analysis of the cross section taken along SQ dimension at the spin state $|\beta\beta\rangle$ in FQ dimension, (C) the combined analysis of the two cross sections from $|\alpha\alpha\rangle$ and $|\beta\beta\rangle$ states of FQ dimension, (D) the combined analysis of the cross sections of states $|\alpha\alpha\rangle$ and $(|\alpha_1\beta_2\rangle + |\beta_1\alpha_2\rangle)/\sqrt{2}$ and $(-|\alpha_1\beta_2\rangle + |\beta_1\alpha_2\rangle)/\sqrt{2}$, (E) the analysis of 1D proton spectrum. Bottom trace: dipolar couplings D_{FH} (D_{15}, D_{16}, D_{25}, D_{26}) and D_{FF} (D_{56}) obtained by the analysis of (D) the combined analysis of the cross sections of states $|\alpha\alpha\rangle$ and $(|\alpha_1\beta_2\rangle + |\beta_1\alpha_2\rangle)/\sqrt{2}$ and $(-|\alpha_1\beta_2\rangle + |\beta_1\alpha_2\rangle)/\sqrt{2}$ and (E) the analysis of 1D proton spectrum. The vertical bars give standard deviations on the parameters determined.

The structural and order parameters of orthodifluorobenzene in the liquid-crystalline solvent have been studied earlier.[41] The main focus of the present study is to develop the methodology to aid the analyses of the complex spectra. Hence, only spectral parameters have been derived, and the molecular geometry and ordering are not reported here.

The study unambiguously establishes that the spin state selective detection of the SQ transitions using MQ coherence not only reduces the complexity of the spectrum drastically but also aids the analysis. The method can therefore be extended to systems with more number of interacting spins. The applica-

tion of this methodology for other complicated systems and to isotropic systems is in progress and will be published elsewhere.

Conclusions

The transitions observed in the SQ spectrum are generally redundant, and all the transitions are not essential for the determination of the spectral parameters. It is shown in the present study that by employing the homonuclear MQ coherence it is possible for spin state selective detection of the SQ transitions on the basis of the spin state of the coupled heteronuclei. The number of transitions excited using this method is significantly less in number than the normal one-dimensional spectrum and is sufficient to determine spectral parameters. Therefore, the analysis of the complex proton spectra is simplified. The technique is demonstrated on the doubly ^{13}C enriched acetonitrile in the liquid-crystalline phase and is applied to the analysis of the complex six-spin proton spectra of orthodifluorobenzene aligned in the liquid-crystalline media.

Acknowledgment. N.S. thanks Department of Science and Technology, New Delhi, for the financial support in the form of research grant No. SR/S1/PC-13/2004. We acknowledge the fruitful discussions with Prof. Anilkumar and Prof. K.V. Ramanathan.

References and Notes

(1) Diehl, P.; Khetrapal, C. L. In *NMR Basic Principles and Progress*; Diehl, P., Fluck, E., Kosfeld, R., Eds.; Springer-Verlag: Berlin, 1969; Vol. 1

(2) Suryaprakash, N. *Concepts Magn. Reson.* **1998**, *10*, 167−192.

(3) Suryaprakash, N. *Curr. Org. Chem.* **2000**, *4*, 85−103.

(4) Christy Rani Grace, R.; Suryaprakash N. In *New Advances in Analytical Techniques;* Rahman, A., Ed.; Harwood Academic Press: The Netherlands, 2000; Vol. 1, pp 441−484.

(5) Christy Rani Grace, R.; Suryaprakash, N.; Kumar, A.; Khetrapal, C. L. *J. Magn. Reson.* **1994**, *107A*, 79−82.

(6) Khetrapal, C. L.; Ramanathan, K. V.; Suryaprakash, N.; Vivekanandan, S. *J. Magn. Reson.* **1998**, *135*, 265−266.

(7) Lu, L.; Nagana Gowda, G. A.; Suryaprakash, N.; Khetrapal, C. L.; Weiss, R. G. *Liq. Cryst.* **1998**, *25*, 295−300.

(8) Field, L. D.; Pierens, G. K.; Carpenter, T. A.; Colebrook, L. D.; Hall, L. D. *J. Magn. Reson.* **1992**, *99*, 398−402

(9) Polson, J. M.; Burnell, E. E. *J. Magn. Res.* **1994**, *A106*, 223−228.

(10) Rendell, J. C. T.; Burnell, E. E. *J. Magn. Res.* **1995**, *A.112*, 1−6.

(11) Chandrakumar, T.; Polson, J. M.; Burnell, E. E. *J. Magn. Res.* **1996**, *A118*, 264−271.

(12) Frydman, L.; Rossomando, P. C.; Frydman, B. *J. Magn. Reson.* **1991**, *95*, 484−494.

(13) Lesot, P.; Ouvrard, J. M.; Ouvrard, B. N.; Courtieu, J. *J. Magn. Reson.* **1994**, *107A*, 141−150.

(14) Nanz, D.; Ernst, M.; Hong, M.; Ziegeweid, M. A.; Schmidt-Rohr, K.; Pines. *J. Magn. Reson.* **1995**, *A113*, 169−176.

(15) Levante, T. O.; Bremi, T.; Ernst, R. R. *J. Magn. Reson.* **1996**, *A121*, 167−177.

(16) Snyder, L. C.; Meiboom, S. Theory of proton NMR with deuteron decoupling in nematic liquid crystalline solvents. *J. Chem. Phys.* **1973**, *58*, 5096−5103.

(17) Vivekanandan, S.; Suryaprakash, N. *Chem. Phys. Lett.* **2001**, *338*, 247−253.

(18) Emsley, J. W.; Merlet, D.; Smith, K. J.; Suryaprakash, N. *J. Magn. Reson.* **2002**, *154*, 303−310.

(19) Vinay Deepak, H. S.; Joy, A.; Suryaprakash, N. *Magn. Reson. Chem.* **2006**, *44*, 553−565.

(20) Vivekanandan, S.; Joy, A.; Suryaprakash, N. *J. Mol. Struct.* **2004**, *694*, 241−247.

(21) Marjanska, M.; Castiglione, F.; Walls, J. D.; Pines, A. *J. Magn. Reson.* **2002**, *158*, 52−59.

(22) Foord, E. K.; Cole, J.; Crawford, M. J.; Emsley, J. W.; Celebre, G.; Longeri, M.; Lindon, J. C. *Liq. Cryst.* **1995**, *18*, 615−621.

(23) Emsley, J. W.; Furby, M. I. C.; De Luca, G. *Liq. Cryst.* **1997**, *21*, 877−883.

(24) Celebre, G.; De Luca, G.; Longeri, M.; Catalano, D.; Lumetti, M.; Emsley, J. W. *Mol. Phys.* **1995**, *85*, 221−231.

(25) Stepehenson, D. S.; Binsch, G. *J. Magn. Reson.* **1980**, *37*, 395−407.

(26) Stepehenson, D. S.; Binsch, G. *Org. Magn. Reson.* **1980**, *14*, 226−233.

(27) Pfandler, P.; Bodenhausen, G. *J. Magn. Reson.* **1991**, *91*, 65−76.

(28) Castiglione, F.; Carravetta, M.; Celebre, G.; Longeri, M. *J. Magn. Reson.* **1998**, *132*, 1−12.

(29) Diehl, P.; Vogt, J. *Org. Magn. Reson.* **1976**, *8*, 638−642.

(30) Diehl, P.; Sykora, S.; Vogt, J. *J. Magn. Reson.* **1975**, *19*, 67−82.

(31) Laatikainen, R.; Niemitz, M.; Weber, U.; Sundelin, J.; Hassinen, T.; Vespäläinen, J. *J. Magn. Reson.* **1996**, *120A*, 1−10.

(32) Inoue, K.; Takeuchi, H.; Konaka, S. *J. Phys. Chem. A* **2001**, *105*, 6711−6716 and references therein.

(33) Sinton, S.; Pines, A. *Chem. Phys. Lett.***1980**, *76*, 263−267.

(34) Warren, W. S.; Pines, A. *J. Am. Chem. Soc.* **1981**, *103*, 1613−1617.

(35) Warren, W. S.; Weitekamp, D. P.; Pines, A. *J. Chem. Phys.* **1980**, *73*, 2084−2099.

(36) Bax, A.; Freeman, R. *J. Magn. Reson.* **1980**, *41*, 507−511.

(37) Braunschweiler, L.; Bodenhausen, G.; Ernst, R. R. *Mol. Phys.* **1983**, *48*, 3, 535−560.

(38) Murali, N.; Ramakrishna, Y. V. S.; Chandrasekhar, K.; Thomas, A. M.; Kumar, A. *Pramana* **1984**, *23*, 547−557.

(39) Diehl, P.; Khetrapal, C. L.; Kellerhals, H. P. *Mol. Phys.* **1968**, *15*, 333−337.

(40) Wray, V.; Ernst, L.; Lustig, E. *J. Magn. Reson.* **1977**, *27*, 1−21.

(41) Väänänen, T.; Jokisaari, J.; Lounila, J. *J. Magn. Reson.* **1982**, *49*, 73−83.